JCSE The Journal of Corrosion Science and Engineering
ISSN 1466-8858 Volume 16, Preprint 42 submitted 13 June 2013

Experimental and quantum studies on corrosion inhibition effect of benzodiazepines on N80 steel in hydrochloric acid

M.Yadav[a]*, Sumit kumar[a], Dipti Sharma[a] and P.N. Yadav[b]

[a]Department of Applied Chemistry, Indian school of Mines, Dhanbad 826004, India
[b]Department of Physics, Post Graduate College Ghazipur, 133002, India
Email: yadav_drmahendra@yahoo.co.in

Abstract

The inhibition effect of synthesized 2, 4-bis (phenyl)-1H-benzodiazepine (BPBD) and 2, 4-bis (methoxyphenyl)-1H-benzodiazepine (BMBD) on corrosion of mild steel in 4M HCl solution was investigated using weight loss measurements, electrochemical polarization and electrochemical impedance spectroscopy (EIS) techniques. The experimental results show that the inhibition efficiency increases as the concentration of the inhibitor was increased. The polarization measurements indicate that the studied inhibitor act as mixed inhibitor. The adsorption of BMBD and BPBD on mild steel surface obey Langmuir adsorption isotherm. The structure of inhibitors were optimized using semi-empirical AM1 method. Quantum chemical parameters such as the highest occupied molecular orbital (E_{HOMO}), lowest unoccupied molecular orbital (E_{LUMO}) energy levels, energy gap ($E_{LUMO} - E_{HOMO}$), dipole moment (μ), global hardness (η), softness (σ), binding energy and the fraction of electrons transferred from the inhibitor molecule to the metal surface (ΔN) were calculated and the adsorption mechanism was discussed. A good correlation between the theoretical data and the experimental results was found. Scanning electron microscopy (SEM) was used to characterize the surface morphology of the mild steel specimens in presence and absence of inhibitors.

Keywords: *N80 steel; EIS; Polarization ; Acid inhibition*

JCSE The Journal of Corrosion Science and Engineering
ISSN 1466-8858 Volume 16, Preprint 42 submitted 13 June 2013

1. Introduction

The N80 steel is widely used as main construction material for downhole tubular, casings, flow lines and transmission pipelines in petroleum industry. In most of the industrial processes, the acidic solutions are commonly used for the pickling, industrial acid cleaning, acid de-scaling, and also widely applied to enhance oil/gas recovery through acidification in the oil and gas industry [1–4]. Acidization of a petroleum oil well is one of the important stimulation techniques for enhancing oil production. It is commonly brought about by forcing a solution of 15% to 28% hydrochloric acid into the well through N80 steel tubing to remove plugging in the bore well and stimulate production in petroleum industry. Unfortunately, tubing steel (N80) get corroded during these acidic applications, which results in terrible waste of both resources and money [5]. To reduce the aggressive attack of the acid on tubing and casing materials (N80 steel), inhibitors are added to the acid solution during the acidifying process. Several methods are used to control the corrosion process but use of corrosion inhibitors is most practical and efficient method for corrosion prevention [6, 7]. Mainly nitrogen, sulfur and oxygen containing compounds like azoles, amines, thioureas, amino acids and their derivatives are reported in the literature as good corrosion inhibitors [8–12]. It is observed that the presence of hetero-atoms (N, S, O), aromatic rings or long alkyl chains generally improves corrosion inhibition efficiency of these compounds [13-16]. The corrosion inhibition efficiency of organic compounds is related to their adsorption properties. Adsorption depends on the nature and the state of the metal surface, nature of corrosive medium and chemical structure of the inhibitor [17]. The effective acidizing inhibitors that are usually found in commercial formulations, suffer from drawbacks because they are effective only at high concentrations and they are harmful to the environment due to their toxicity [18-20] , so it is important to search for new nontoxic and effective organic corrosion

ISSN 1466-8858 Volume 16, Preprint 42 submitted 13 June 2013

inhibitors for N80 steel – 15% HCl system. The choice of these compounds was based on the consideration that they contain good π-electron conjugation, enhancing its coordination, and an abundance of heteroatoms, enhancing its adsorption on the surface of mild steel. Further it was intended to study the influence of substitution of $–OCH_3$ group on the inhibition efficiencies.

Keeping in view the importance of organic compounds as corrosion inhibitors, we synthesized 2, 4-bis (phenyl)-1H-benzodiazepine (BPBD) and 2, 4-bis (methoxyphenyl)-1H-benzodiazepine (BMBD) and studied their corrosion inhibition properties using weight loss measurement, potentiodynamic polarization, electrochemical impedance spectroscopy (EIS) and quantum chemical calculation methods.

2. Experimental Procedure

2.1. Materials

2.1.1 N80 steel sample

The corrosion studies were performed on N80 steel samples with a composition (wt. %): C, 0.31; Mn, 0.92; Si, 0.19; S, 0.008; P, 0.010; Cr, 0.20 and Fe balance. The N80 Steel coupons having dimension 6.0 cm × 2.5 cm × 0.1 cm size were mechanically cut and abraded with different grade emery papers (120, 220, 400, 600, 800, 1500 and 2000 grade) for weight loss experiment. For Electrochemical measurements mild steel coupons having dimension 1.0 cm × 1.0 cm × 0.1 cm were mechanically cut and abraded with same manner as before, with an exposed area of 1 cm^2 (rest covered with araldite resin) with 3 cm long stem. Prior to the experiment, specimens were washed with distilled water, degreased in acetone, dried and stored in vacuum desiccator.

JCSE The Journal of Corrosion Science and Engineering
ISSN 1466-8858 Volume 16, Preprint 42 submitted 13 June 2013

2.1.2 Test Solutions

For weight loss and electrochemical studied, the test solutions (15% HCl, wt %) were prepared by dilution of analytical grade 37% HCl (Ramkem) with double distilled water. The concentrations of the studied inhibitors ranged from 50 ppm to 250 ppm by weight in 15% HCl solution.

2.1.3 Synthesis of corrosion inhibitor

The compounds BPBD and BMBD were synthesized by the reaction of 4-methoxyacetophenone, 4-substututed benzaldehyde and o-phenylenediamine by the reported method [21] as shown is Scheme 1.The structure of the compound was confirmed by spectroscopic techniques and purity was checked by thin layer chromatography.The purity of the synthesized compounds were confirmed by thin layer chromatography.The structure of BPBD and BMBD are shown in Fig.1.

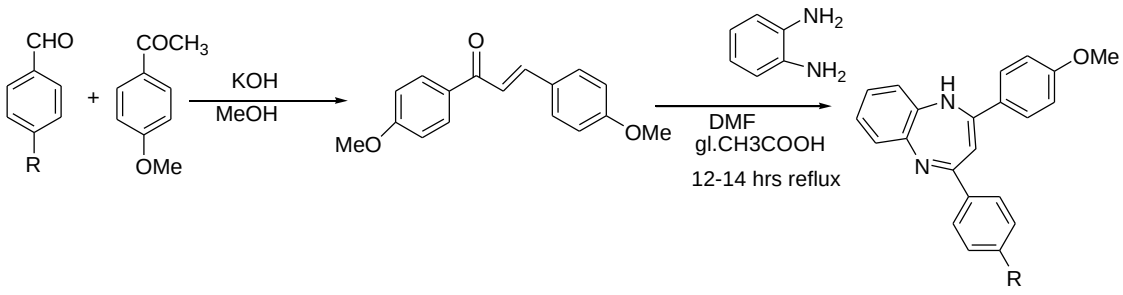

R = -OMe, H

Scheme 1: Synthetic route of inhibitors: (a) BMBD (b) BPBD.

JCSE The Journal of Corrosion Science and Engineering
ISSN 1466-8858 Volume 16, Preprint 42 submitted 13 June 2013

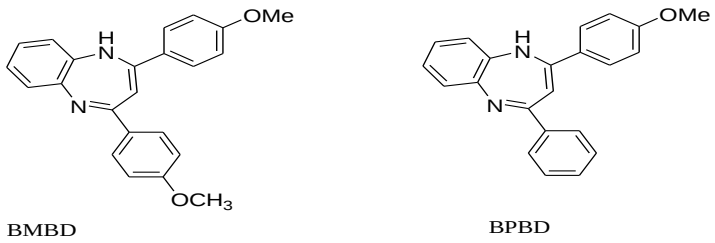

Fig. 1: Structure of inhibitors: (a) BMBD (b) BPBD.

2.2. Methods

2.2.1. Weight loss method

Weight loss measurements were performed by immersing accurately weighed mild steel test coupons in 250 mL of 15% HCl in absence and in the presence of 50, 100, 150, 200 and 250 ppm (mgL^{-1}) of the inhibitors. The immersion time was optimized and optimized immersion time (6 h) was uniformly used for weight loss measurements. The test coupons were then removed from the electrolyte, washed thoroughly with distilled water, dried and weighed. Triplicate experiments were conducted for each concentration of the inhibitor for the reproducibility and the average of weight losses were taken to calculate the corrosion rate and inhibition efficiency of the inhibitors. The corrosion rate (*CR*), inhibition efficiency (η%) and surface coverage (θ) were determined by following equations [22]:

$$CR\left(mmy^{-1}\right) = \frac{87.6W}{Atd} \qquad (1)$$

where W = weight loss, A = area of specimen in cm^2 exposed in acidic solution, t = immersion time in hours, and d = density of N80 steel (g cm^{-3}).

$$\theta = \frac{CR_0 - CR_i}{CR_0} \quad (2)$$

$$\eta(\%) = \frac{CR_0 - CR_i}{CR_0} \times 100 \quad (3)$$

where CR_0 and CR_i are corrosion rate in absence and presence of inhibitors. This experiment was repeated at different temperature of 30, 40, 50 and 60 ˚C by using water circulated Ultra thermostat (model NBE, Germany) to determine the temperature dependence of the inhibition efficiency.

2.2.2. Electrochemical studies

Electrochemical polarization measurements were carried out in a conventional three-electrode cell consisting of N80 steel working electrode (WE), a platinum counter electrode (CE) and a saturated calomel electrode (SCE) as reference electrode, using CH electrochemical workstation (Model No: CHI 760D, manufactured by CH Instruments, Austin, USA) at 30 ºC. Before starting the experiments, the working electrodes were immersed in the test solution for 30 min until a steady potential reached. The N80 steel surface was exposed (1cm^2) to various concentrations (50-200 ppm) of different inhibitors in 150 mL of 15% HCl at 30 ºC. After establishment of the open circuit potential, dynamic polarization curves were obtained with a scan rate of 1 mV/s in the potential range from -700 to +300 mV. Corrosion current density (i_{corr}) values were obtained by Tafel extrapolation method. All potentials were measured against SCE. The percentage inhibition efficiency (η %), was calculated using the equation

$$\eta(\%) = \frac{i^0_{corr} - i_{corr}}{i^0_{corr}} \times 100 \quad (4)$$

where, i^0_{corr} and i_{corr} are the values of corrosion current density in absence and presence of inhibitors, respectively.

JCSE The Journal of Corrosion Science and Engineering
ISSN 1466-8858 Volume 16, Preprint 42 submitted 13 June 2013

Impedance measurements were carried out using the same electrochemical cell and electrochemical workstation as mentioned above in the frequency range from 0.1 to 10000 Hz using amplitude of 10 mV peak to peak with an ac signal at the open-circuit potential. The impedance data were obtained by using Nyquist plots. The charge-transfer resistance (R_{ct}) values were calculated from the difference in impedance at low and high frequencies. The inhibition efficiency (η %) was calculated from charge transfer resistance values obtained from impedance measurement according to the following relation:

$$\eta(\%) = \frac{R_{ct(inh)} - R_{ct}}{R_{ct(inh)}} \times 100 \qquad (5)$$

where $R_{ct(inh)}$ *and* R_{ct} are charge transfer resistance in presence and absence of inhibitor respectively. The values of electrochemical double layer capacitance (C_{dl}) were calculated at the frequency f_{max}, at which the imaginary component of the impedance is maximal ($-Z_i$) in the Niquist plots by using the following equation [23]:

$$C_{dl} = \frac{1}{2\pi f_{max} R_{ct}} \qquad (6)$$

2.2.3. Scanning electron microscopic (SEM) analysis

In order to observe the changes in surface morphologies of corrosive samples before and after the addition of inhibitor, the N80 steel specimens were immersed in 15% HCl solutions in the absence and presence of optimum concentration of inhibitor for 6 h at 30 ºC. After immersion for 6 h the steel specimens were taken out from the solution and cleaned with distilled water, dried using a cold air blaster, and then the surface was investigated by a JSM-5800, MODEL S-3400N scanning electron microscope (SEM).

2.2.4. Quantum chemical study

Quantum chemical calculations were carried out by using semi- empirical AM1 method because this method is highly reliable for calculating the physical properties of molecules from the program package HYPERCHEM 8.0. All the calculations were carried out with the help of complete geometry optimization. Polak-Ribiere algorithm was used with RMS gradient of 0.1 kcal $Å^{-1}mol^{-1}$ for the semi-empirical calculation. Theoretical parameters such as the highest occupied molecular orbital (E_{HOMO}), lowest unoccupied molecular orbital (E_{LUMO}) energy levels, energy gap ($E_{LUMO} - E_{HOMO}$), dipole moment (μ), global hardness (η), softness (σ), binding energy, molecular surface area and the fraction of electrons transferred from the inhibitor molecule to the metal surface (ΔN) were calculated.

3. Results and Discussion

3.1. Weight loss measurements

Corrosion inhibition efficiency (η %) of inhibitors (BPBD, BMBD) calculated by weight loss measurements after 6 h of immersion time at 303 K are given in Table 1. The data in Table 1 reveal that inhibition efficient increases with increase in concentration for each inhibitor up to 200 ppm and becomes almost constant at 250 ppm. The increase in inhibition efficiency with increasing concentration of inhibitors is due to increase in the surface coverage, resulting retardation of metal dissolution [24]. The inhibition efficiency of inhibitors follow the order: BMBD >BPBD. Corrosion inhibition studies were also carried out at different temperatures ranging from 303K to 333K. Corrosion parameters namely corrosion rate (CR), surface coverage (θ) and inhibition efficiency (η %) obtained from weight loss measurements at different temperatures are shown in Table 1. The data in Table 1 reveal that the maximum efficiency of 96% was obtained for BMBD in presence of 250 ppm at 303 K. The corrosion rates were much less in presence of inhibitors [25] as compared to in absence of inhibitors.

JCSE The Journal of Corrosion Science and Engineering
ISSN 1466-8858 Volume 16, Preprint 42 submitted 13 June 2013

The data in Table 1 reveal that the inhibition efficiency decreases with increasing temperature [26]. Such type of behavior can be described on the basis that the increase in temperature leads to a shift of the equilibrium constant towards desorption of the inhibitors molecules at the surface of N80 steel.

3.1.1. Thermodynamic and activation parameters

Thermodynamic and activation parameters play an important role in understanding the inhibitive mechanism. The weight loss measurements were done in the temperature range of 303-333 K in the absence and presence of different concentrations of inhibitors (BPBD, BMBD) in 15% HCl for N80 steel. The apparent activation energy (E_a) for dissolution of mild steel in 15% HCl can be expressed by Arrhenius equation:

$$\log CR = \frac{-E_a}{2.303RT} + \log A \qquad (7)$$

Where CR is the corrosion rate, E_a is the apparent activation energy, R is the molar gas constant (8.314 J $K^{-1}mol^{-1}$), T is the absolute temperature (K) and A is the Arrhenius pre-exponential factor.

Fig.1 represents the Arrhenius plot of log CR against 1/T for the corrosion process of N80 steel in 15% HCl solution in the absence and presence of inhibitors (BPBD, BMBD) at concentrations ranging from 50 ppm to 250 ppm. From Fig.2, the slope of each individual line was determined and activation energy was calculated by using the slope value (E_a = (slope) × 2.303 × R) and the calculated value of E_a were summarized in Table 2. It is evident from Table 2 that, the values of E_a were higher for inhibited solutions as compared to the uninhibited solutions indicating that the energy barrier for the corrosion reaction increases due to physical adsorption of the inhibitors on the metal surface [27]

JCSE The Journal of Corrosion Science and Engineering
ISSN 1466-8858 Volume 16, Preprint 42 submitted 13 June 2013

Table 1 : Corrosion parameters namely corrosion rate(*CR*), surface coverage (θ) and inhibition efficiency η (%) of N80 steel in 15%HCl in the presence and absence of inhibitor at different temperature, obtained from weight loss measurements

Conc. (ppm)	**303 K**			**313 K**			**323 K**			**333 K**		
	CR (mmy^{-1})	θ	η %	*CR* (mmy^{-1})	θ	η %	*CR* (mmy^{-1})	θ	η %	*CR* (mmy^{-1})	θ	η %
BMBD												
Blank	20.20	-	-	34.55	-	-	55.47	-	-	92.69	-	-
50	3.11	0.84	84.6	6.66	0.80	80.7	13.47	0.75	75.7	27.80	0.70	70.0
100	2.36	0.88	88.3	5.18	0.85	85.0	10.87	0.80	80.4	22.48	0.75	75.2
150	1.69	0.91	91.6	3.76	0.89	89.1	8.43	0.84	84.8	18.72	0.79	79.8
200	1.15	0.94	94.3	2.97	0.91	91.4	6.93	0.87	87.5	15.66	0.83	83.1
250	0.80	0.96	96.0	2.28	0.93	93.4	5.76	0.89	89.6	13.71	0.85	85.2
BPBD												
50	3.57	0.82	82.3	7.56	0.78	78.1	14.64	0.73	73.6	30.58	0.67	67.0
100	2.66	0.86	86.8	5.76	0.83	83.3	11.60	0.79	79.1	25.21	0.72	72.8
150	2.08	0.89	89.7	4.42	0.87	87.2	9.15	0.83	83.5	20.76	0.77	77.6
200	1.45	0.92	92.8	3.66	0.89	89.4	7.71	0.86	86.1	17.98	0.80	80.6
250	1.09	0.94	94.6	2.79	0.92	91.9	6.48	0.88	88.3	15.75	0.83	83.0

.

JCSE The Journal of Corrosion Science and Engineering
ISSN 1466-8858 bmitted 13 June 2013

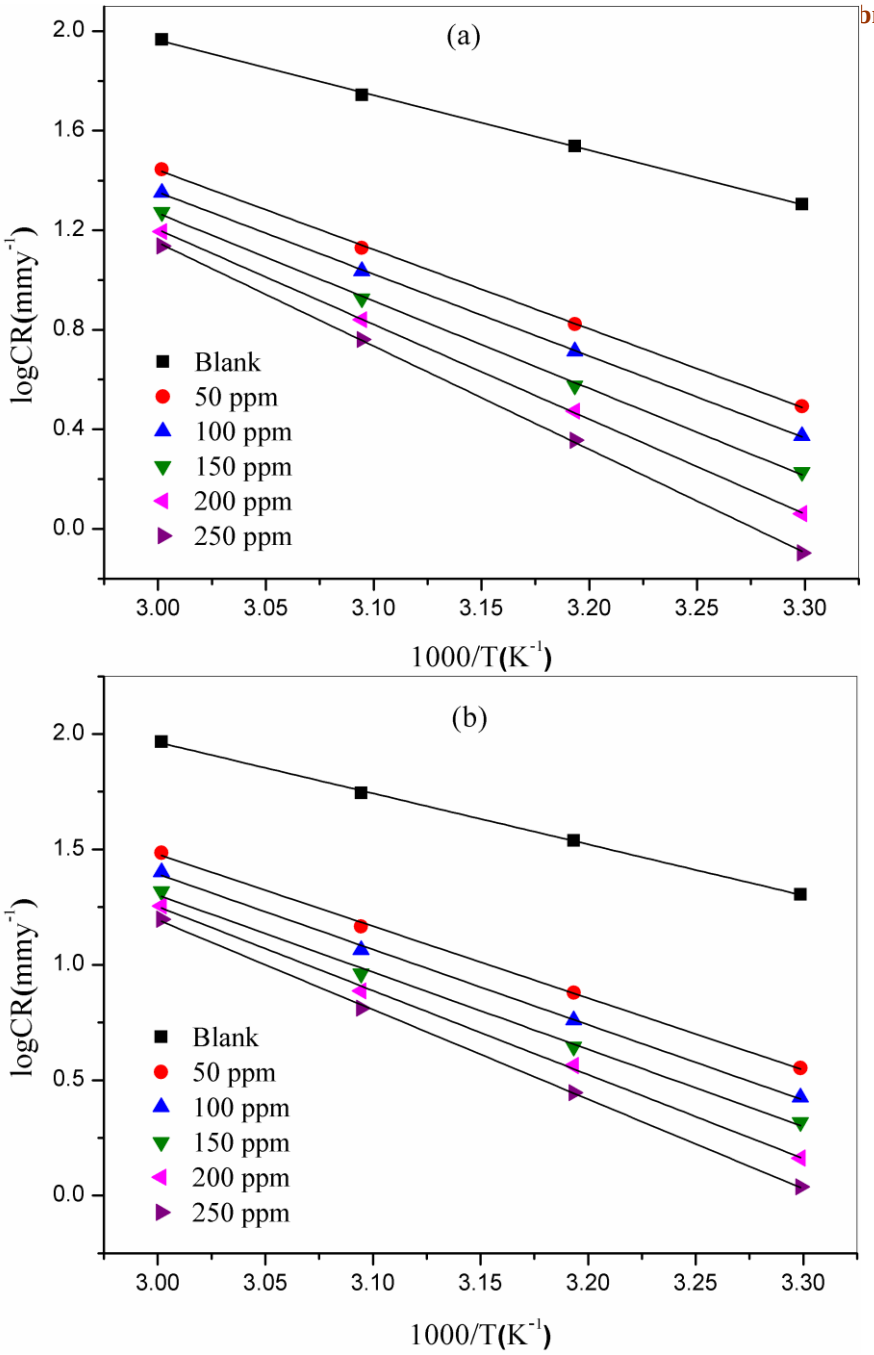

Fig. 2. Arrhenius plots for N80 steel corrosion in 15% HCl (a) BMBD (b) BPBD

JCSE The Journal of Corrosion Science and Engineering
ISSN 1466-8858 Volume 16, Preprint 42 submitted 13 June 2013

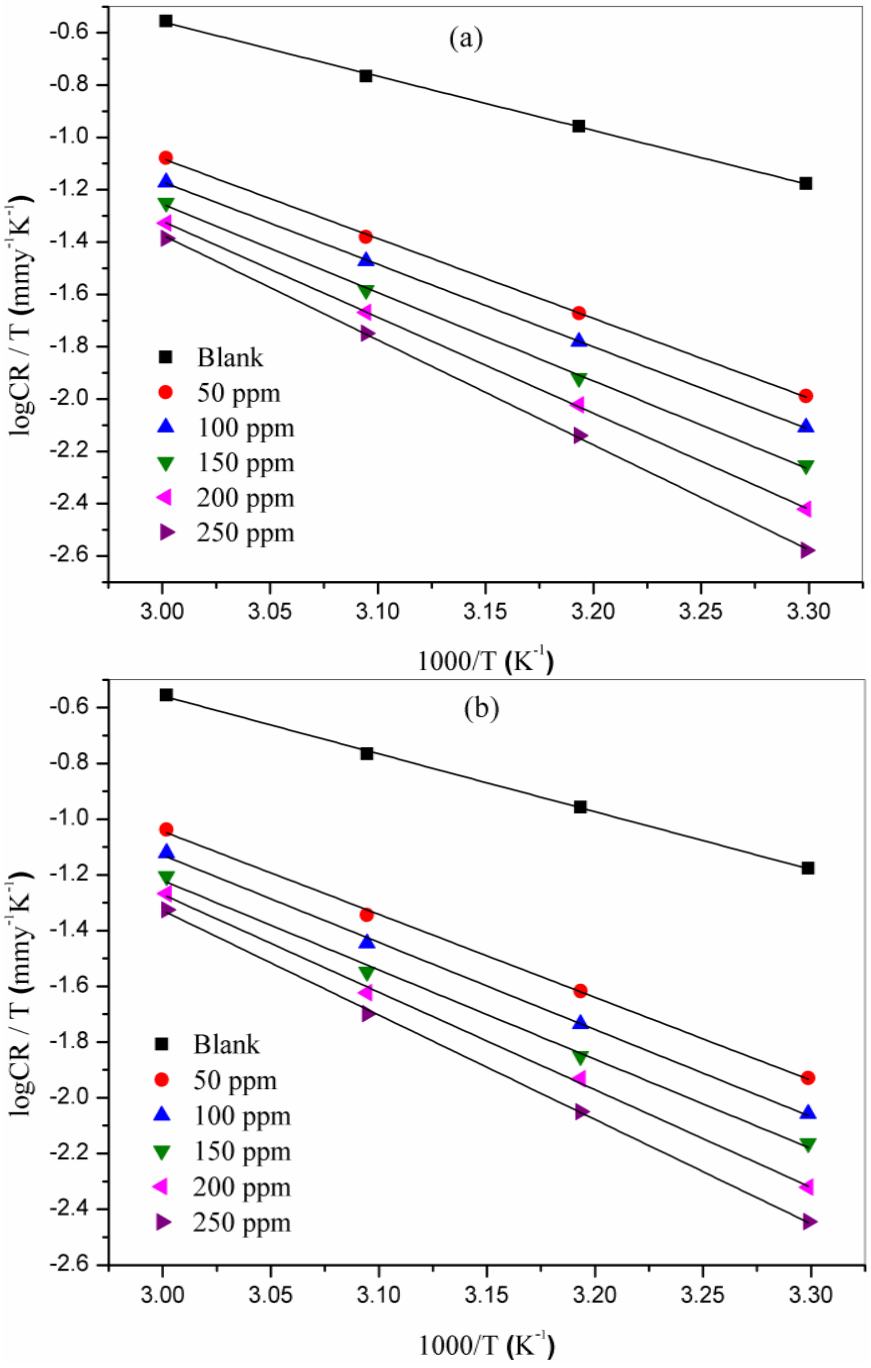

Fig.3. Transition state plot for N80 steel in 15% HCl at different concentration (a) BMBD (b) BPBD.

The relationships between the temperature dependence of percentage inhibition efficiency (η %) of an inhibitor and the E_a can be classified into three groups according to temperature effects [28].

JCSE The Journal of Corrosion Science and Engineering
ISSN 1466-8858 Volume 16, Preprint 42 submitted 13 June 2013

(i) η % decreases with increase in temperature, E_a (inhibited solution) > E_a (uninhibited solution) (ii) η % increases with increase in temperature, E_a (inhibited solution) < E_a (uninhibited solution) (iii) η % does not change with temperature, E_a (inhibited solution) = E_a (uninhibited solution)

In the present investigation both the inhibitors follows the second group (i) where E_a (inhibited solution) > E_a (uninhibited solution), and E_a increases with inhibitor concentration, which further confirm η % decreases with increase in temperature.

The values of standard enthalpy of activation (ΔH^*) and standard entropy of activation (ΔS^*) can be calculated by using the equation:

$$CR = \frac{RT}{Nh}\exp\left(\frac{\Delta S^*}{R}\right)\exp\left(-\frac{\Delta H^*}{RT}\right) \qquad (8)$$

where, CR is the corrosion rate, ΔH^* is the enthalpy of activation, ΔS^* is the entropy of activation, h is Planck's constant and N is the Avogadro number, respectively.

Table 2. Activation parameter for N80 steel in 15% HCl solution in the absence and presence of inhibitor obtained from weight loss measurements.

Inhibitor	Concentration (ppm)	E_a (kJmol^{-1})	ΔH^* (kJ/mol)	ΔS^* (Jmol^{-1}K^{-1})
Blank	-	42.34	39.70	-89.20
	50	61.08	58.44	-43.05
BMBD	100	63.00	60.36	-39.03
	150	67.33	64.69	-27.54
	200	72.93	70.29	-12.04
	250	79.45	76.80	6.53
BPBD	50	59.63	56.99	-46.69
	100	62.50	59.85	-39.80
	150	64.60	61.36	-36.93
	200	69.69	67.04	-20.84
	250	74.34	71.70	-8.01

A Plot of log (*CR* /T) against 1/T (Fig. 3) gave straight lines with slope of (-Δ*H**/2.303*R*) and intercept of (log R/Nh + Δ*S**/2.303R) from which the activation thermodynamic parameters (Δ*H** and Δ*S**) were calculated and listed in Table 2. The positive sign of the enthalpy reflects the endothermic nature of the N80 steel dissolution process [29, 30]. The negative value of ΔS^* for both the inhibitors indicates that activated complex in the rate determining step represents an association rather than a dissociation step, meaning that a decrease in disorder takes place during the course of transition from reactant to the activated complex [3].

3.1.2. Adsorption isotherm

Basic information on the interaction between the organic inhibitors and the N80 steel surface are obtained from various adsorption isotherms. The most commonly used adsorption isotherms are Langmuir, Temkin, and Frumkin isotherm. The surface coverage (θ) for different concentrations of inhibitors in 15% hydrochloric acid was tested graphically for fitting a suitable adsorption isotherm. Plotting C_{inh}/θ vs. C_{inh} yielded a straight line [Fig. 4] with a correlation coefficient (r^2) values 0.998, 0.999 for BPBD and BMBD respectively at 303K. This indicates that the adsorption of these inhibitors can be fitted to a Langmuir adsorption isotherm represented by the following equation.

$$\frac{C_{inh}}{\theta} = \frac{1}{K_{ads}} + C_{inh} \qquad (9)$$

where, C_{inh} is the inhibitor concentration, K_{ads} is the equilibrium constant for adsorption-desorption process. The slope values for both the inhibitors were also found to be very near to unity confirming the validity of Langmuir adsorption isotherms. From the intercept of Fig.4 the values of K_{ads} were calculated. Large values of K_{ads} obtained for all the three studied inhibitors suggesting strong adsorption and hence better corrosion inhibition efficiency. Using the values of K_{ads} the values of ΔG°_{ads} were calculated by using the following equation:

JCSE The Journal of Corrosion Science and Engineering
ISSN 1466-8858 Volume 16, Preprint 42 submitted 13 June 2013

$$\Delta G^0_{ads} = -RT\ln(55.5K_{ads}) \quad (10)$$

where R is the gas constant and T is the absolute temperature (K). The value of 55.5 is the concentration of water in solution in mol L^{-1}. Calculated values of K_{ads} and ΔG°_{ads} are listed in Table 3. It is apparent from the Table 3 that the Calculated values of ΔG°_{ads} lies between -35.24 to -37.82 kJ mol^{-1} and -36.23 to -38.26 kJ mol^{-1} for BPBD and BMBD respectively in the temperature range 303 to 333 K. The negative values of $\Delta G°_{ads}$ indicate a spontaneous adsorption process and stability of the adsorbed film of inhibitors on N80 surface [32].

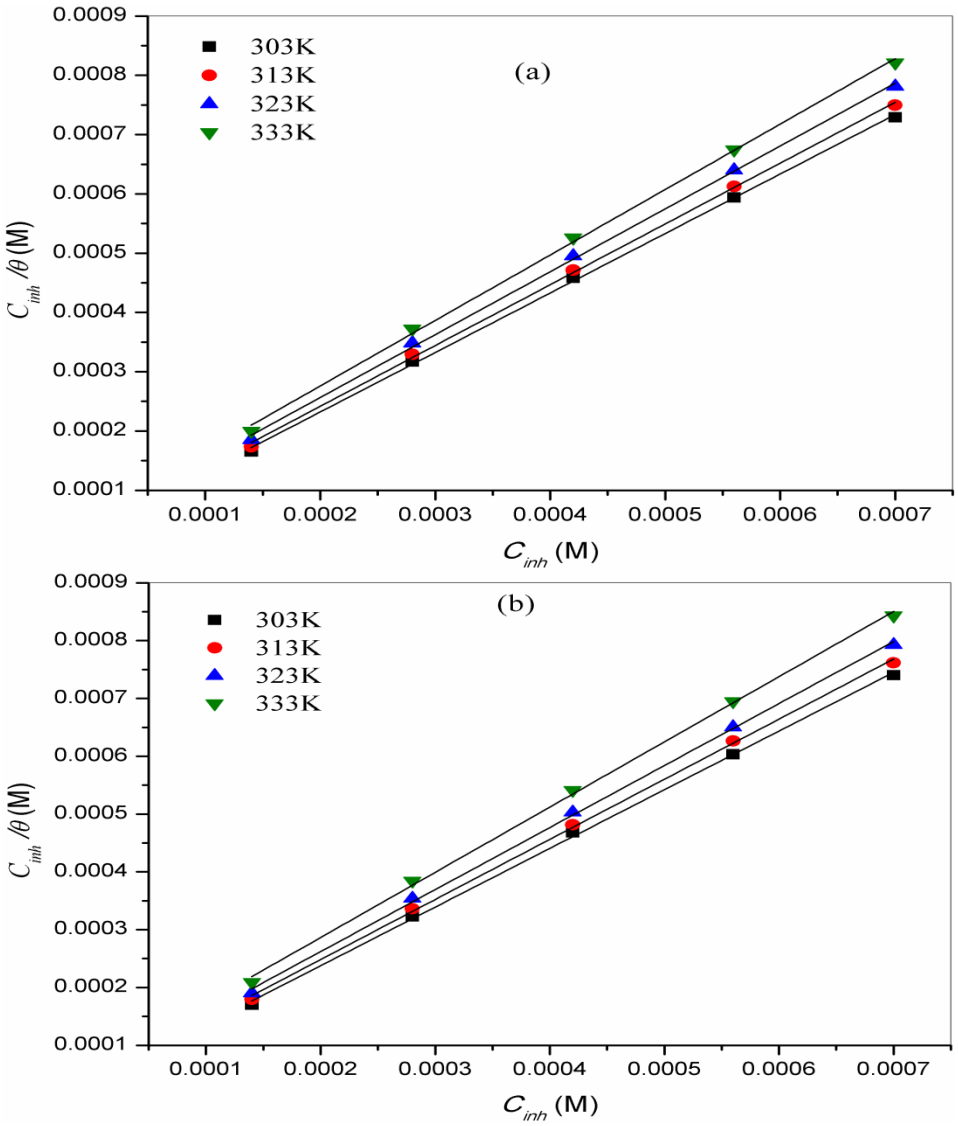

Fig. 4. Langmuir plots for (a) BMBD (b) BPBD.

JCSE The Journal of Corrosion Science and Engineering
ISSN 1466-8858 Volume 16, Preprint 42 submitted 13 June 2013

Table 3. Adsorption parameters for BMBD and BPBD calculated from Langmuir adsorption isotherm for N80 steel in 15% HCl solution at 303-333 K.

Inhibitor	Temperature (K)	K_{ads} (M^{-1})	ΔG°_{ads} (kJ mol^{-1})
BMBD	303K	3.1×10^{4}	-36.23
	313K	2.7×10^{4}	-37.02
	323K	2.2×10^{4}	-37.69
	333K	1.8×10^{4}	-38.26
BPBD	303K	2.8×10^{4}	35.24
	313K	2.4×10^{4}	36.78
	323K	2.1×10^{4}	-37.51
	333K	1.6×10^{4}	-37.82

It is generally accepted that for the values of $\Delta G°_{ads}$ upto – 20 kJ/mol, the type of adsorption were regarded as physisorption; the inhibition occurs due to the electrostatic interactions between the charged molecules of the inhibitors and the charged metallic surfaces, while the values above - 40 kJ/mol were reported as chemisorption, which occurs due to the charge sharing or a transfer from the inhibitors molecules to the metal surface to form a covalent bond [33, 34].The values of $\Delta G°_{ads}$ in our measurements suggested that the adsorption is neither typical physisorption nor typical chemisorption but it is complex mixed type adsorption involving both physisorption and chemisorptions [35].

3.2. Potentiodynamic polarization measurements

The anodic and cathodic polarization curves for the corrosion of N80 steel in 15% HCl in the presence and absence of varying concentrations of inhibitors (BPBD,BMBD) at 303K are shown in Fig.5. The corrosion current densities and corrosion potentials were calculated by extrapolation of linear parts of cathodic and anodic curves to the point of inter section. The electrochemical parameters such as corrosion potential (E_{corr}), corrosion current density (i_{corr}),

ISSN 1466-8858 Volume 16, Preprint 42 submitted 13 June 2013

anodic Tafel slope (b_a) and cathodic Tafel slope (b_c) and percentage inhibition efficiency (η %) determined from polarisation curves are summarized in Table 4. The data in Table 4 clearly show that the current density decreases in the presence of inhibitors (BPBD, BMBD), this indicated that inhibitors adsorbed on the metal surface and hence the inhibition efficiency increases with the increase in the inhibitor concentrations. It is apparent from the Fig.5 that the nature of the polarization curves remain the same in the absence and presence of inhibitors but the curves shifted towards lower current density in presence of inhibitors. It concluded that the inhibitors molecules retard the corrosion process without changing the mechanism of corrosion process in the medium of investigation.

The presence of inhibitors cause small change in E_{corr} value. This implies that the inhibitor acts as a mixed type inhibitor, affecting both anodic and cathodic reactions [36]. If the displacement in E_{corr} is more than ±85 mV/SCE relating to corrosion potential of the blank, the inhibitor can be considered as a cathodic or anodic type [37]. If the change in E_{corr} is less than 85 mV the corrosion inhibitor may be regarded as a mixed type. The maximum displacement in our study is less than 20 mV/SCE, which indicates that BPBD and BMBD act as mixed type inhibitor. However the minor shift of E_{corr} values towards positive direction on increasing the concentration of inhibitors suggesting the predominant anodic control over the reaction.

JCSE The Journal of Corrosion Science and Engineering
ISSN 1466-8858 Volume 16, Preprint 42 submitted 13 June 2013

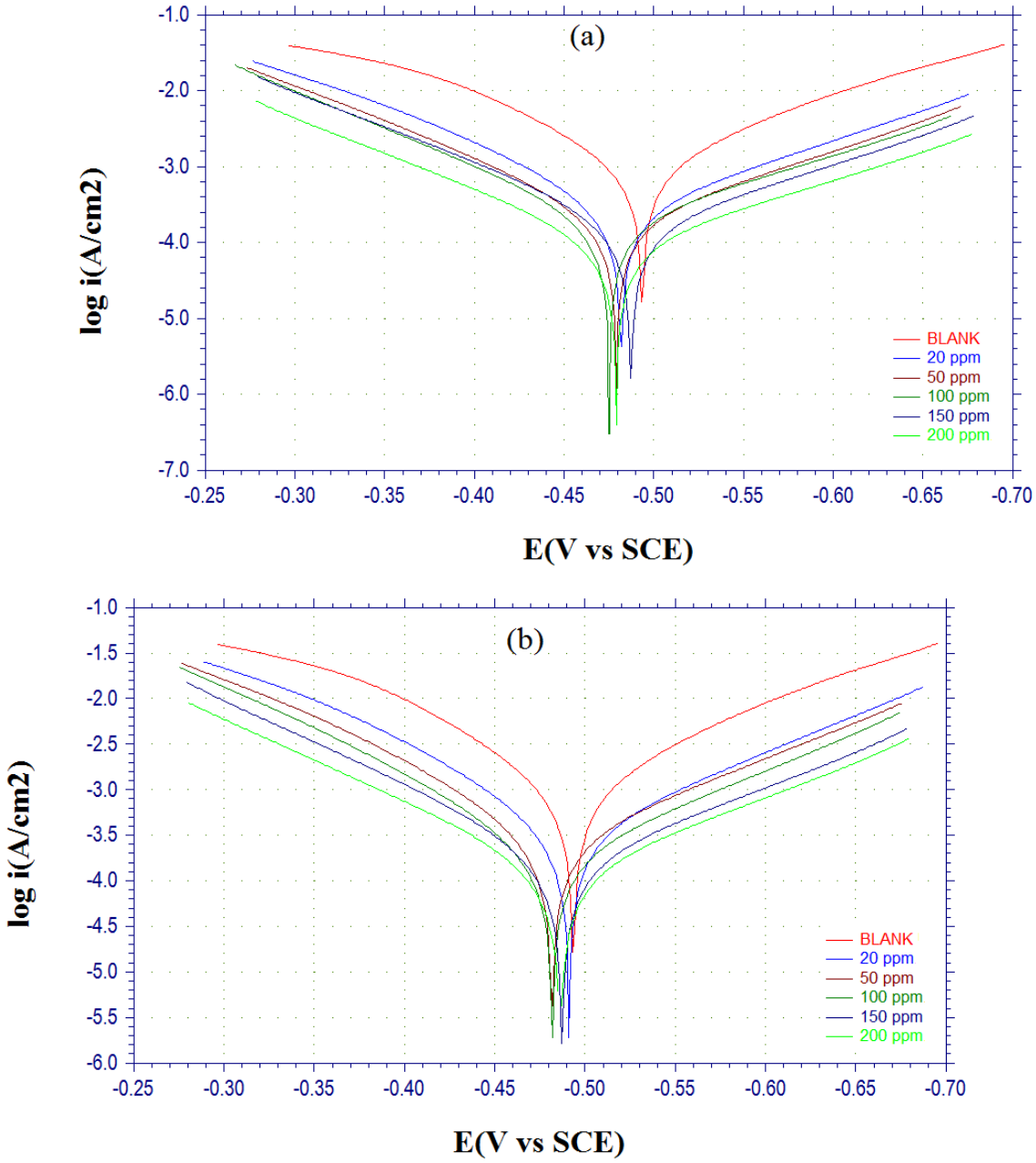

Fig. 5. Potentiodynamic polarization curves for N80steel in 15% HCl in the presence and absence of inhibitor at 303K. (a) BMBD (b) BPBD.

JCSE The Journal of Corrosion Science and Engineering
ISSN 1466-8858 Volume 16, Preprint 42 submitted 13 June 2013

Table 4.Electrochemical parameter and percentage Inhibition efficiency (η %) obtained from polarization and impedance studies for N80 steel in 15% HCl solution in the presence or absence of inhibitor at 303 K.

Conc.	Tafel extrapolation data					EIS data		
(ppm)	E_{corr} (V vs SCE)	b_a (mV dec^{-1})	b_c (mV dec^{-1})	I_{corr} (μAcm^{-2})	η %	R_{ct} (Ω cm^2)	C_{dl} (μF cm^2)	η %
BMBD								
Blank	-495	93	142	568	-	20	252	-
50	-492	51	104	84.0	85.2	120	146	83.4
100	-490	69	86	63.6	88.8	148	122	86.5
150	-487	81	97	42.6	92.5	253	104	92.1
200	-485	57	168	25.0	95.6	285	94	93.0
BPBD								
50	-493	94	127	96.5	83.2	107	102	81.3
100	-491	71	83	77.8	86.3	153	83	87.0
150	-488	55	102	53.9	90.5	202	72	90.1
200	-486	90	98	37.5	93.4	273	63	92.7

3.3. Electrochemical impedance spectroscopy (EIS)

Nyquist plot of N80 steel in 15% HCl solution in absence and presence of different concentrations of BPBD and BMBD at 303K are shown in Fig.6. It follows from Fig.6 that a high frequency depressed charge-transfer semicircle was observed. The charge transfer resistance (R_{ct}) and double layer capacitance (C_{dl}) obtained from the Nyquist plots and the calculated inhibition efficiency values (η %) are shown in Table 4.

ISSN 1466-8858 Volume 16, Preprint 42 submitted 13 June 2013

It is apparent from the Table 4 that the value of R_{ct} increases on increasing the concentration of the inhibitors.The increase in R_{ct} values is attributed to the formation of an insulating protective film at the metal/solution interface.

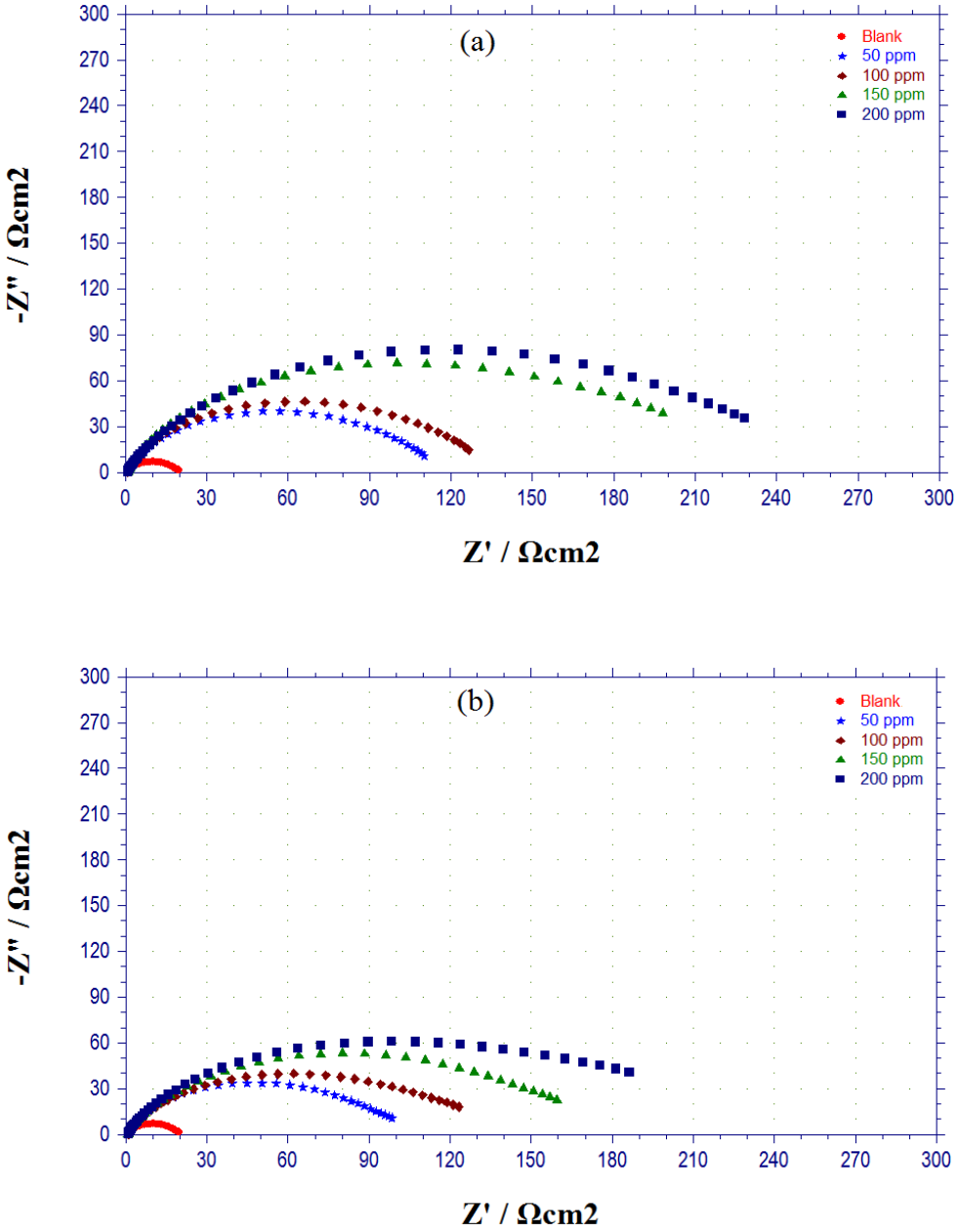

Fig. 6. Nyquist plot for N80 steel in 15% HCl acid containing various concentrations of (a) BMBD(b) BPBD at 303K.

It is also clear that the value of C_{dl} decreases on the addition of inhibitors, indicating a decrease in the local dielectric constant and/or an increase in the thickness of the electrical double layer, suggesting the inhibitor molecules function by the formation of the protective

layer at the metal surface [38]. This type of behavior can be generalized and explained by Helmholtz model given in Eq. (11) [39].

$$C_{dl} = \frac{\varepsilon\varepsilon_0 A}{d} \qquad (11)$$

where ε is the dielectric constant of the medium, ε_0 is the permittivity of the free space; A is the effective surface area of the electrode, d is the thickness of the protective double layer formed by inhibitors.

So, the changes in R_{ct} and C_{dl} values were caused by the steady replacement of the water molecules by adsorption of inhibitor on mild steel surface, reducing the extent of metal dissolution [40]. Both the electrochemical method (polarization measurement and EIS study) offered nearly same trend.

3.4. Scanning electron microscopy (SEM)

The surface morphology of the N80 steel samples in 15% HCl solution in the absence and in the presence of 250 ppm of BPBD and BMBD are shown in Figs. 7 (a, b c, d). The badly damaged surface obtained when the metal was kept immersed in 15% HCl solution for 6 h without inhibitor indicates significant corrosion. However, in presence of inhibitors the surface has remarkably improved with respect to its smoothness indicating considerable reduction of corrosion rate. This improvement in surface morphology is due to the formation of a good protective film of inhibitor on N80 steel surface which is responsible for inhibition of corrosion.

JCSE The Journal of Corrosion Science and Engineering
ISSN 1466-8858 Volume 16, Preprint 42 submitted 13 June 2013

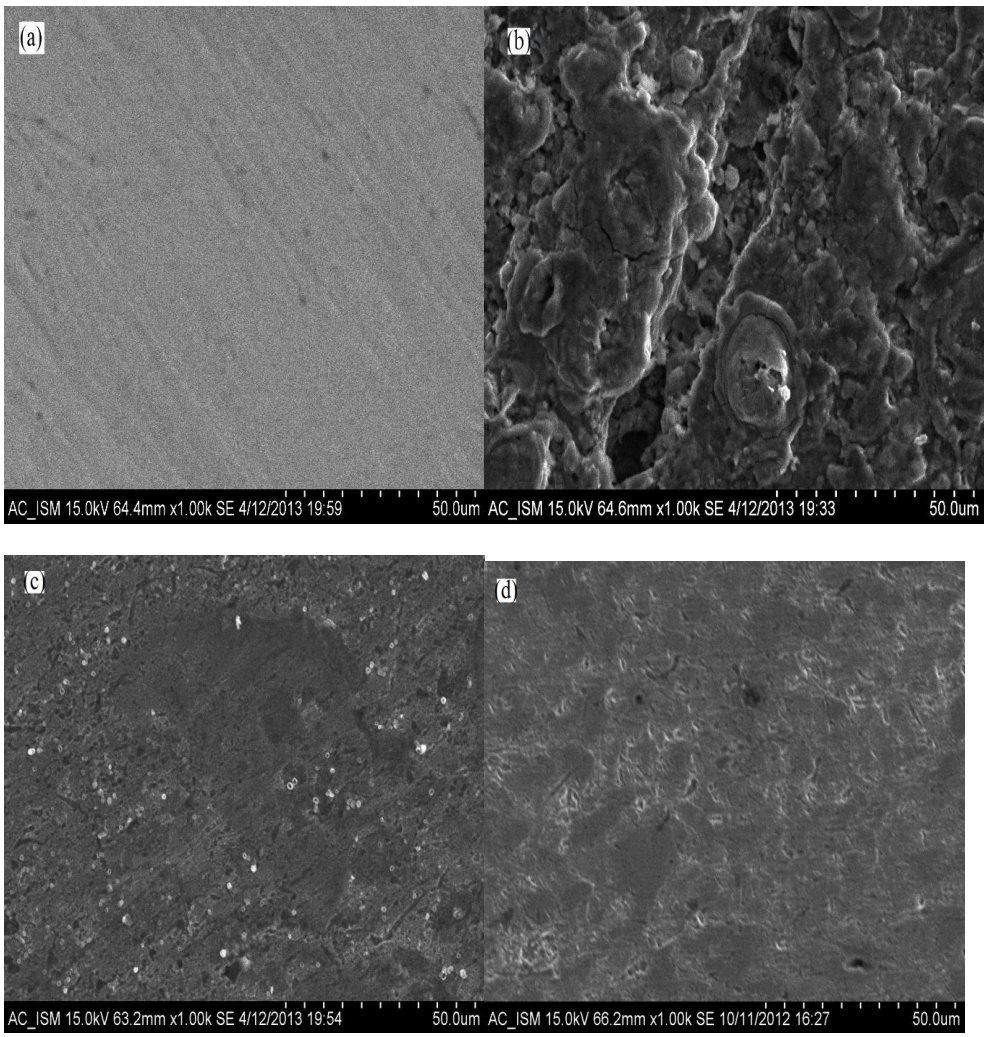

Fig.7. SEM image of N80 steel in 15% HCl solution after 6 h immersion at 303K (a) before immersion (polished) (b) After immersion without inhibitor (c) in presence of inhibitor BMBD(d) in presence of inhibitor BPBD.

3.5. Theoretical calculation

In order to study the effect of molecular structure on the inhibition efficiency, quantum chemical calculations were performed by using semi-empirical AM1 method and all the calculations were carried out with the help of complete geometry optimization. Optimized structure, E_{HOMO} and E_{LUMO} are shown in Fig. 8. The frontier molecular orbital energies (E_{HOMO} and E_{LUMO}) are significant parameters for the prediction of the reactivity of a chemical species. The E_{HOMO} is often associated with the electron donating ability of a

molecule. The inhibition efficiency increases with the increasing E_{HOMO}, values. High E_{HOMO} values indicate that the molecule has a tendency to donate electrons to appropriate acceptor molecules with low energy empty molecular orbital. The lower value of E_{LUMO}, suggesting that the molecule easily accepts electrons from the donor molecules [41, 42]. It was reported previously by some researchers that smaller values of ΔE and higher values of dipole moment (μ) are responsible for enhancement of inhibition efficiency [43, 44].The quantum chemical parameters such as the energy of the highest occupied molecular orbital (E_{HOMO}), the energy of the lowest unoccupied molecular orbital (E_{LUMO}), energy gap ($\Delta E = E_{LUMO} - E_{HOMO}$), the dipole moment ($\mu$), absolute electronagativity (χ), global hardness (η), softness (σ), binding energy, molecular surface area and the fraction of electrons transferred from the inhibitor molecule to the metal surface (ΔN) were calculated and summarized in Table 5. For the calculations of quantum chemical parameters the following equations were used [45-47]:

$$\chi = -\frac{E_{LUMO} + E_{HOMO}}{2} \quad (12)$$

$$\eta = \frac{E_{LUMO} - E_{HOMO}}{2} \quad (13)$$

The inverse of the global hardness is designated as the softness, σ as follows:

$$\sigma = \frac{1}{\eta} \quad (14)$$

where, hardness and softness are the properties to measure the molecular stability and reactivity. Hard molecule has large energy gap and a small gap exist in soft molecule. Soft molecules are more reactive than hard ones because they can offer electron to acceptors easily. For the simplest transfer of electrons, adsorption could occur at the part of the molecule where σ which is a local property, has the highest value [46].

JCSE The Journal of Corrosion Science and Engineering
ISSN 1466-8858 Volume 16, Preprint 42 submitted 13 June 2013

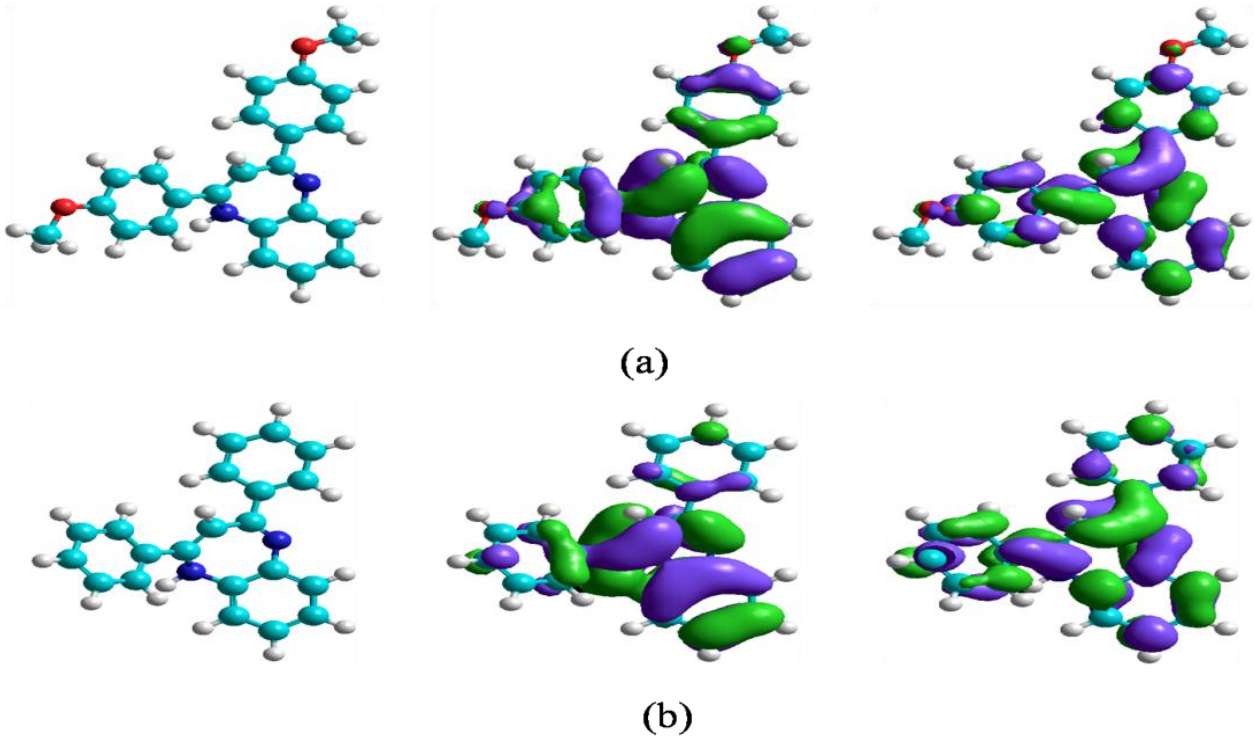

Fig.8. The optimized structure (left) and HOMO (center) and LUMO (right) distribution for molecules (a) BMBD (b) BPBD.[Atom legend: white = H; Cyan = N; blue = N; red = O]

Table 5. Quantum chemical parameters for different inhibitors.

Inhibitor	E_{HOMO} (eV)	E_{LUMO} (eV)	ΔE (eV)	μ (D)	η (eV)	σ (eV)	ΔN (e)	Binding energy (kcalmol^{-1})	Molecular surface area(Å^2)
BMBD	-8.1448	-0.5775	7.5673	3.171	3.7837	0.2643	0.2875	-4520.26	559.07
BPBD	-8.2241	-0.4979	7.7262	2.798	3.8631	0.2586	0.2612	-4465.32	519.23

It is reported by Kokaji [48] that the work function (Φ) of metal surface is an appropriate measure of its electronegativity and should be used together with its vanishing absolute hardness to estimate the ΔN as given below:

$$\Delta N = \frac{\Phi - \chi_{inh}}{2\eta_{inh}} \qquad (15)$$

According to the result obtained from the Table 5, the highest value of E_{HOMO} (-8.1448eV) and lowest values of ΔE (7.5673 eV) are found for BMBD. It can be affirmed that BMBD has more potency to get adsorbed on the mild steel surface than BPBD. For our present investigation the inhibition efficiency increases with the increasing dipole moment of the inhibitors. In literature some degree of confusion exists when dealing with dipole momentum data interpretation where some authors reported positive [49,50] and some reported negative [51,52] relationship between μ and inhibition efficiency. From our present investigation BMBD is having highest value of σ (0.2643 eV) has the highest efficiency (Table 5) which is good in agreement with experimental data. Generally ΔN shows inhibition efficiency resulted by electron transferred from the inhibitor molecule to the iron atom [41]. According to Lukovits's study [46], if the value of ΔN is < 3.6, the efficiency of inhibition increases with increasing electron donating ability of the inhibitor at the metal surface. An improvement in electronic releasing power was shown by replacing hydrogen atom by electron donating substituent ($-OCH_3$ group) which improves the inhibition efficiency. In this study, it can be seen from Table 5 that the ability to donate electrons to the metal surface follows the order of BMBD > BPBD, which is in good agreement with the order of inhibition efficiency of these inhibitors.

The high negative values of binding energy obtained for all the three inhibitors (Table 5) indicates the stability of the adsorbed inhibitor molecules which cannot be split or broken

apart from metal surface easily. Molecular surface area (a geometrical quantity) determines various properties of inhibitor molecules, as it interact through their surface residue. It has been found that the large surface area values obtained for all studied inhibitors (Table 5) attributed to the uniformity of coverage of the surface of the N80 steel [53].The most negative value of binding energy and largest molecular size of BMBD (Table 5) indicating its highest inhibition efficiency.

4. CONCLUSIONS

(1) The synthesized benzodiazepine derivatives show good inhibition efficiencies for the corrosion of N80 steel in 15% HCl solutions and the inhibition efficiency increases on increasing the concentration of these inhibitors and with the increase in temperature. The order of inhibiting performance of the inhibitors is: BMBD > BPBD.

(2) The variation in the values of b_a and b_c (Tafel slopes) and the minor deviation of E_{corr} with respect to E (corrosion potential of the blank) indicate that both the tested inhibitors are mixed type in nature.

(3) EIS measurements show that charge transfer resistance (R_{ct}) increases and double layer capacitance (C_{dl}) decreases in presence of inhibitors, suggested the adsorption of the inhibitor molecules on the surface of N80 steel.

(4) It is suggested from the results obtained from SEM and Langmuir adsorption isotherm that the mechanism of corrosion inhibition is occurring mainly through adsorption process.

(5) The experimental inhibition efficiencies of three inhibitors are closely related to the quantum chemical parameters E_{HOMO}, E_{LUMO}, ΔE and σ.

ISSN 1466-8858 Volume 16, Preprint 42 submitted 13 June 2013

Reeferences

[1]. G.E. Badr, *Corros. Sci.*, 51, 2529 (2009).

[2]. Vishwanatham and P.K. Sinha, *Anti-Corrosion Methods and Materials*., 56, 139 (2009).

[3]. V. R. Saliyan and A. V. Adhikari, *Bull. Mater. Sci.*, 31 ,699 (2008).

[4]. A. Kosari, M. Momeni, R. Parvizi, M. Zakeri, M.H. Moayed, A. Davoodi and H. Eshghi, *Corros. Sci.*, 53, 3058 (2011).

[5]. S. Deng and X. Li, *Corros. Sci.*, 55, 407 (2012).

[6]. N. Hackerman, *Langmuir*, 3, 922 (1987).

[7]. P.G. Cao, J.L. Yao, J.W. Zheng, R.A. Gu and Z.Q. Tian, *Langmuir*, 18, 100 (2002).

[8]. M. Yadav and U. Sharma, (**2012**) Arab J Chem, DOI: 10.1016/arabjc.2012.03.011.

[9]. M. Yadav and U. Sharma, *J.* Mater. *Environ. Sci.*, 2, 407 (2011).

[10]. M. Yadav and U. Sharma, *Corros. Eng. Sci. Technol*., 48, 19 (2013).

[11]. M.M. Singh and R.B. Rastogi, *Mater. Chem. Phys.*, 80, 283 (2003).

[12]. K. Babic-Samardzija, C. Lupu, N. Hackerman and A.R. Barron, *J. Mater. Chem*., 15, 1908 (2005).

[13]. D. Turcio-Ortega, T. Pandiyan, J. Cruz and E. Garcia-Ochoa, *J. Phys. Chem.* C , 111, 9853 (2007).

[14]. E.E. Oguzie, S.G. Wang, Y. Li and F.H. Wang, *J. Phys. Chem.* C, 113, 8420 (2009).

[15]. R.C. Ayers Jr. and N. Hackerman, *J. Electrochem. Soc.* , 110, 507 (1963).

[16]. C. Jeyaprabha, S. Sathiyanarayanan, K.L.N. Phani and G. Venkatachari, *J. Electroanal. Chem.*, 585, 250 (2005).

[17]. S. Ghareba and S. Omanovic, *Corros. Sci.*, 52, 2104 (2010).

[18]. M. Ozcan , I. Dehri and M. Erbil, *Appl. Surf. Sci.* , 236 , 155 (2004).

[19]. K. D. Neemla, A. Jayaraman, R. C. Saxena, A.K. Agrawal and R. Krishna, *Bulletien of Electrochemistry*, 5, 250-253.

[20]. W. W. Frenier, F. B. Growcock and V. R. Lopp, *Corrosion*, 44, 590 (1988).

[21]. S. B. Jadhav, Int. J. Pharm. Sci., 3, 181 (2011).

[22]. G. Shukla, S. K. Dwivedi, P. Sundaram and S. Prakash, *Ind. Eng. Chem. Res.*, 50, 11954 (2011).

[23]. H. A. Sorkhabi, B. Shaabani and D. Seifzdeh *Appl.Surf. Sci.*, 239, 154 (2005).

[24]. A. U. Ezeoke1, O. G. Adeyemi1, O. A. Akerele1 and N. O. Obi-Egbedi, *Int. J. Electrochem. Sci.*, 7, 534 (2012).

[25]. E. E. Ebenso and I. B. Obot, Inhibitive Properties, *Int. J. Electrochem. Sci.*, 5, 2012 (2010).

[26]. L. F. Mar, O. O. Xometl, A. Marco, P. A. Lozada and F. J. Cruz , *Corros. Sci*., 61, 171 (2012).

[27]. E.E. Oguzie, Corros. Sci., 50, 2993 (2008).

[28]. A. R. S. Priya, V. S. Muralidharam and A. Subramania, *Corrosion*., 64, 541 (2008).

[29]. A. Popova, E. Sokolova, S. Raicheva and M. Chritov, *Corros. Sci.*, 45, 33 (2003).

[30]. G. Quartarone, G. Moretti, A. Tassan and A. Zingales,. *Mater. Corros.*, 45, 641 (1994).

[31]. S. V. Ramesh and S. V. Adhikari, *Bull. Mater. Sci*., 31, 699 (2007).

[32]. J. D. Talati and D. K. Gandhi, *Corros. Sci.*, 23, 1315 (1983).

[33]. Z. Szklarska-Smialowska and J. Mankowski, *Corros. Sci*., 18, 953 (1978).

[34]. A. Yurt, S. Ulutas and H. Dat, *Appl. Surf. Sci*., 253, 919 (2006).

[35]. S. K. Shukla and M.A. Quraishi, *Corros. Sci*., 51, 1990 (2009).

[36]. D. Jayaperumal, *Mater. Chem. Phys.*, 119, 478 (2010).

ISSN 1466-8858 Volume 16, Preprint 42 submitted 13 June 2013

[37]. E. S. Ferreira, C. Giancomlli, F. C. Giacomlli and A. Spinelli, *Mater. Chem. Phys*., 83, 129 (2004).

[38]. I. Ahamad, R. Prasad and M. A. Quraisi, *Corros. Sci*., 52, 1472 (2010).

[39]. C. Bataillon and S. Brunet, *Electrochim. Acta*., 39, 455 (1994).

[40]. B. Trachli, M. Keddam, H. Takenouti and A. Srhiri,. *Corros. Sci.*, 44, 997 (2002).

[41]. S. Xia, M. Qiu, L. Yu, F. Liu and H. Zhao, *Corros. Sci*., 50, 2021 (2008).

[42]. E.E. Ebenso, T. Arslan, F. Kandemirli, N. Caner and I. Love, *Int. J. Quantum. Chem.*, 110, 1003 (2010).

[43]. Y.M. Tang, W.Z. Yang, X.S. Yin, Y. Liu, R. Wan and J.T. Wang,. *Chem. Phys.*, 116, 479 (2009).

[44]. D. Q. Zhang, Q. Y. Pan, L. X. Gao and G. D. Zhou, *Corros. Sci.*, 48, 1437 (2006).

[45]. V. S. Sastri and J. R. Perumareddi, *Corrosion (NACE).*, 53, 617 (1997).

[46]. I. Lukovits, E. Klaman and F. Zucchi, *Corrosion (NACE).*, 57, 3 (2001)

[47]. G. Pearson, *J. Org. Chem*., 54, 1423 (1989).

[48]. A. Kokaji, surfaces. *Chem. Phys.* 2012, 393, p 1-12.

[49]. A. Stoyanova, G. Petkova and S.D. Peyerimhoff, *Chem. Phys*., 279, 1 (2002).

[50]. O. Benali, L. Larabi, M. Traisnel, L. Gengembre and Y. Harek, *Appl. Surf. Sci.*, 253, 6130 (2007).

[51]. G. Gao and C. Liang, *Electrochim. Acta.*, 52, 4554 (2007).

[52]. I. B. Obot, N. O. ObiEgbedi and S. A. Umoren, *Corros. Sci.*, 51, 276 (2009)–282.

[53]. I. B. Obot and N. O. ObiEgbedi, Surf. Rev. Lett., 15, 903 (2008).